Biologia (2024) 79:937–952
https://doi.org/10.1007/s11756-023-01589-y

ORIGINAL ARTICLE

Antibacterial activity of mixed metal oxide derived from Zn-Al layered double hydroxide precursors, effect of calcination temperature

Fethi Ghribi[1,2,3] · Tayeb Bouarroudj[1] · Youcef Messai[4] · Ilyas Belkhattab[5] · Abdelmounaim Chetoui[5] · Amira Bourouba[6] · Amina Bourouba[6] · Houneida Benbouzid[6] · Okba Louafi[7] · Abdelghani Djahoudi[8] · Zoubir Benmaamar[2] · Khaldoune Bachari[1]

Received: 30 July 2023 / Accepted: 12 December 2023 / Published online: 12 January 2024
© The Author(s), under exclusive licence to Plant Science and Biodiversity Centre, Slovak Academy of Sciences (SAS), Institute of Zoology, Slovak Academy of Sciences (SAS), Institute of Molecular Biology, Slovak Academy of Sciences (SAS) 2024

Abstract

For several decades, the use of antibiotics has led to the emergence of highly resistant human and animal pathogens, posing a significant threat to global health, food security, and economic progress. In the quest for alternatives to combat multidrug-resistant bacteria and yeasts, the utilization of nanoparticles materials has emerged as a promising avenue. In this research, we investigated the antimicrobial properties of Zn-Al-layered double hydroxide, synthesized through co-precipitation and subsequently calcined at temperatures of 400, 600, and 800°C. A total of 21 bacterial strains, including 15 clinical strains and 6 Gram-reference strains, along with one fungal strain, were subjected to testing. The synthesized materials underwent characterization using various techniques such as X-ray diffraction (XRD) spectroscopy, scanning electron microscopy (SEM), ultraviolet–visible spectroscopy, and fourier-transform infrared (FTIR) spectroscopy. The key findings indicate that the uncalcined Zn-Al-layered double hydroxide and the heterojunction ZnO-$ZnAl_2O_4$ calcined at 400°C and 600°C exhibited a minimum inhibitory concentration (MIC) of 0.125 µg/mL against the tested strains. The spinell $ZnAl_2O_4$ calcined at 800°C showed MICs ranging between 0.125 and 2 µg/mL, with a greater bactericidal effect on gram-negative bacteria (GNBs) such as Enterobacteriaceae and non-Enterobacteriaceae compared to Gram-positive bacteria. Consequently, the heterojunction ZnO-$ZnAl_2O_4$ demonstrated higher efficacy against Gram-positive bacteria. These findings highlight the potential of heterojunction ZnO-$ZnAl_2O_4$ and spinell $ZnAl_2O_4$ as mixed metal oxides derived from ZnAl-layered double hydroxide, offering promising alternatives to traditional antibiotics and suggesting their potential use as impregnating agents in matrices with a broad spectrum of specific antimicrobial activity.

Keywords Layered Double Hydroxide (LDHs) · Mixed metal oxide (MMO) · ZnO-$ZnAl_2O_4$ · Antimicrobial Activity · Minimum Inhibitory Concentration (MIC) · Minimum Bactericidal Concentration (MBC)

Abbreviations

S.M	Supplementary material
XRD	X-ray Diffraction Spectroscopy
FTIR	Fourier-Transform Infrared Spectroscopy.
SEM	Scanning Electron Microscopy
UV–Vis	Ultraviolet Visible Spectroscopy

✉ Okba Louafi
louafiokba7@gmail.com

[1] Scientific and Technical Research Center in Physico-Chemical Analyses (CRAPC), BP 384, RP42004 Bou-Ismail, Tipaza, Algeria

[2] Energy Processes and Nanotechnology Laboratory, Blida1 University, Blida, Algeria

[3] Laboratory of Functional Analysis of Chemical Processes, Blida1 University, Blida, Algeria

[4] Laboratory for the Study of Surfaces and Interfaces of Solid Matter (LESIMS), Badji Mokhtar University, 23000 Annaba, Algeria

[5] Research Center in Semiconductors Technology for Energetic (CRTSE), 02 Bd Frantz Fanon, Les 07Merveilles BP: 140, 16038 Algiers, Algeria

[6] Laboratory of Cellular Toxicology, Department of Biology, Faculty of Sciences, University of Badji Mokhtar, 23000 Annaba, Algeria

[7] Department of Material Sciences, Faculty of Exact Sciences and Natural and Life Sciences Echahid Cheikh Larbi Tebessi University Tebessa, Constantine Road, 12002 Tebessa, Algeria

[8] Laboratory of Microbiology, Department of Pharmacy, Faculty of Medicine, University of Badji Mokhtar, 23000 Annaba, Algeria

NPs	Nanoparticles
ROS	Reactive Oxygen Species
LDH	Layered Double Hydroxide
MMO	Mixed Metal Oxide
MIC	Minimum Inhibitory Concentration
MBC	Minimum Bactericidal Concentration
GNB	Gram-negative bacteria
ATCC	American Type Culture Collection
CFU	Colony Forming Unit
PCD	Programmed Cell Death

Introduction

The incorrect utilization of antimicrobials has resulted in the emergence of strains that exhibit resistance to multiple drugs. Consequently, this has led to an escalation in the occurrence of infectious diseases and fatalities. Bacterial resistance can arise from genetic alterations that transpire as bacteria adapt to their surroundings, or through the process of horizontal gene transfer (HGT).(Derewacz et al. 2013; Silva et al. 2019). Antibacterial agents play a crucial role in preventing the proliferation of microorganisms and minimizing their adverse effects on our daily lives. (Zhao et al. 2018). A lot of illness, death, and economic stress is caused by nosocomial infections (Revelas 2012). Improper utilization of antimicrobial agents in clinical settings is a key factor contributing to the emergence of alarming diseases. This misuse leads to the development of bacteria that exhibit resistance to multiple drugs and possess an extended lifespan. The rapid proliferation of these drug-resistant bacteria is a major cause for concern (Fymat 2017; MacGowan and Macnaughton 2017). As public health awareness regarding the detrimental impacts of various microbes continues to rise, there is an increasing need for antibacterial materials across various sectors. These materials are sought after in medical devices, hospital supplies, surgical equipment, household sanitation products, textiles, as well as in food packaging and storage.(Vallapa et al. 2011; Vinet and Zhedanov 2011; Pan et al. 2019). The modification of materials with the incorporation of antimicrobial activity is highly desirable to reduce the risk of contamination (Vinet and Zhedanov 2011). Given this concern, utilizing nanomaterials as antimicrobial agents is a logical approach. Nanomaterials offer advantages in scenarios where antibiotics may be ineffective. They can achieve this through various mechanisms, including the disruption of microbial membranes, prevention of biofilms formation, and simultaneous targeting of multiple pathways to impede microbial growth. Notably, the mechanisms by which bacteria develop resistance to antibiotics often differ from the mechanisms employed by nanomaterials.(Wang et al. 2017; Silva et al. 2019). Extensive research has been dedicated to solid bactericidal materials due to their exceptional bactericidal activity and structural durability. As a result, these materials have gained widespread usage in various applications. (Lin et al. 2009; Salem et al. 2015).

Currently, inorganic antimicrobial agents, including metal salts, nano-sized metals, and metal oxides, show great potential and promise (Ibrahim et al. 2013; Petkova et al. 2014). CuO, TiO_2, CeO_2, SiO_2, Fe_3O_3, Al_2O_3, and ZnO are all metal oxides that are often used as antibacterial agents (Nath et al. 2016; Ibrahim et al. 2017; Zhao et al. 2018). Furthermore, the synergistic properties observed in composite metal oxides have surpassed those of individual oxides, leading to significant advancements in this rapidly evolving scientific field(Stankic et al. 2016; Bayahia et al. 2017; Chakra et al. 2017). Over the past few years, there has been notable progress in the development of zinc oxides derived from the hydrothermal treatment of layered double hydroxide (LDH) structures. These novel materials exhibit remarkable optical properties. By leveraging the larger band gap of ZnAl2O4 (Eg = 3.8 eV) compared to ZnO (Eg = 3.37 eV), scientists have successfully engineered an LDH-derived material with enhanced UV absorbance, surpassing that of pure ZnO. (Dai et al. 2018; Ghribi et al. 2020). Layered double hydroxides (LDHs) are a class of anionic clays composed of stacked layers. These layers consist of various cations and different amounts of counter ions positioned between them. Each LDH layer comprises octahedral units, denoted as M(OH)6, which are connected through shared edges, resembling the structure of brucite. These octahedral units contain both M2 + and M3 + ions, with the positively charged M3 + units experiencing electrostatic repulsion, causing them to remain dispersed and avoid proximity to one another. This characteristic ensures the distribution of metal ions throughout the LDH layers. (Kanezaki 2004; Lin et al. 2009).

In our research, we employed the chemical co-precipitation method for the synthesis of our materials. Subsequently, the obtained material underwent varying calcination temperatures (400, 600, and 800 °C) to explore the impact of this factor on its structure. Samples obtained at different calcination temperatures were then subjected to a range of characterizations, encompassing X-ray diffraction (XRD) for structural analysis, scanning electron microscopy (SEM) for morphological analysis, UV–visible spectroscopy for optical analysis, and Fourier transform infrared spectroscopy (FTIR) for infrared analysis. These characterizations enabled us to gain a holistic understanding of the structural, morphological, optical, and infrared properties of our study material at different calcination temperatures.

Furthermore, the antibacterial activities of the synthesized nanomaterials were evaluated against 21 multidrug-resistant bacteria, comprising both Gram-positive and Gram-negative strains. The testing involved ATCC reference strains such as Enterococcus faecalis ATCC 29212, Staphylococcus ATCC 29213, Staphylococcus aureus ATCC 25923, Staphylococcus aureus ATCC 43300, Bacillus ATCC 16404, Pseudomonas

aeruginosa ATCC 27853, and Salmonella typhi ATCC 14028. Additionally, clinical strains including Acinetobacter baumannii MDR-05, Acinetobacter NDM, Acinetobacter OXA23, Bacillus cereus, Escherichia coli B.L.S.E, Escherichia coli M.C.R.1, Elizabethkingia anophelis, Klebsiella oxytoca, Klebsiella pneumoniae carbapenemase-negative (Kpc-), Klebsiella pneumoniae carbapenemase-positive (Kpc +), Pseudomonas VIM-2, Serratia marcescens, Sphingomonas, Staphylococcus aureus cipro, as well as a fungal strain Candida albicans were included in the evaluation. The antibacterial testing was conducted in the absence of light.

Materials and methods

Chemicals and bacterial strains

The chemicals used were obtained from Sigma-Aldrich. The General Microbiology Laboratory at the Faculty of Medicine at Badji Mokhtar University in Annaba, which is supervised by Professor DJAHOUDI A.E.G., was kind enough to supply the bacterial strains that were used in this study.

Preparation of ZnAl—layered double hydroxide (LDHs)

Materials were prepared via co precipitation method at pH value of 9—10. The synthesis was carried out by a slow addition of two metal nitrates solutions (Zn $(NO_3)_2.6H_2O$) and Al $(NO_3)_3.9H_2O$ with Zn/Al molar ratios of 2. The solution that contained 1 M of sodium nitrate ($NaNO_3$) was added slowly (drop wise addition) to the metal nitrates solutions with constant stirring. The pH value for all samples was controlled by addition of aqueous NaOH (2 M). The resulting slurry was aged at 80 C° for 24 h in an oil bath shaker. The precipitate was washed with deionized water many times with centrifugation. Finally, the precipitate was dried in an oven at 80 C° for 18 h. The resultant ZnAl-layered double hydroxide was ground into fine powder. A quantity of the materials was calcined at 400 °C, 600 °C and 800 °C for 5 h to get ZnAl-400 and ZnAl-600 and ZnAl-800. Scheme 1(S.M).

Characterization of ZnAl –LDH and ZnAl-mixed metal oxide (MMO)

Different methods were used to characterize the prepared samples. The structural characterization was carried out using the Siemens D-5000 diffractometer with Cu-Ka radiation (k = 1.5418 Å) in 2θ range of 5–80°. Scanning Electron Microscopy (SEM: JEOL-JSM-6390) was used to appreciate the morphological observations. The UV–Vis absorption spectra were measured by a UV–Vis spectrophotometer (Shimadzu UV-2401). The Infrared Spectra (FTIR) was scanned in the range of 400–4000 cm-1 using a JASCO-FTIR-4200 spectrophotometer.

Determination of minimum inhibitory concentration (MIC)

The minimum inhibitory concentration (MIC) represents the lowest concentration completely inhibiting visible bacterial growth after 24 h of incubation at 37°C(Curcic et al. 2012; Obeizi et al. 2021). The MIC of ZnAl-LDH and ZnAl-MMO was determined by the micro dilution method. At 37°C for 18 h, gram-positive and gram-negative bacteria were cultured on nutrient agar. The inoculums of organisms should be prepared at 105 CFU/ mL Prepared solutions of our material have concentrations of (512, 256, 128, 64, 32, 16, 8, 4, 2, 1, and 0.5 µg/ mL), followed by sonication and autoclaving at 121 °C for 30 min. 2 ml of each concentration were mixed with 18 ml of Muller Hinton agar for 30 min), then the plates were incubated at 37°C for 18–24 h.

Determination of minimum bactericidal concentration (MBC)

The minimum bactericidal concentration (MBC) is usually found by figuring out the MIC and then trying to grow alive organisms that have been exposed to drug concentrations above the MIC in media that doesn't kill bacteria. Most of the time, a 3 log10 (99.9%) drop in the number of viable cells is taken as the point at which the organism has been completely wiped out. This is because complete sterilization of cultures is not an easily attainable endpoint(O'Neill and Chopra 2004).

Determination of the MBC / MIC ratio

Xenobiotic with a MBC/MIC ratio ≤ 4 are defined as bactericidal, while a MBC/MIC ratio > 4 indicates bacteriostatic activity and is tolerant when the ratio is > 26(Zabransky et al. 1973; O'Neill and Chopra 2004).

Results and discussions

Characterizations of ZnAl LDH and ZnAl MMO

XRD analysis

The XRD patterns of the final products of uncalcined ZnAl-LDH and calcined at 400, 600, and 800°C for 5 h are presented in Fig. 1. The XRD pattern relative to the uncalcined

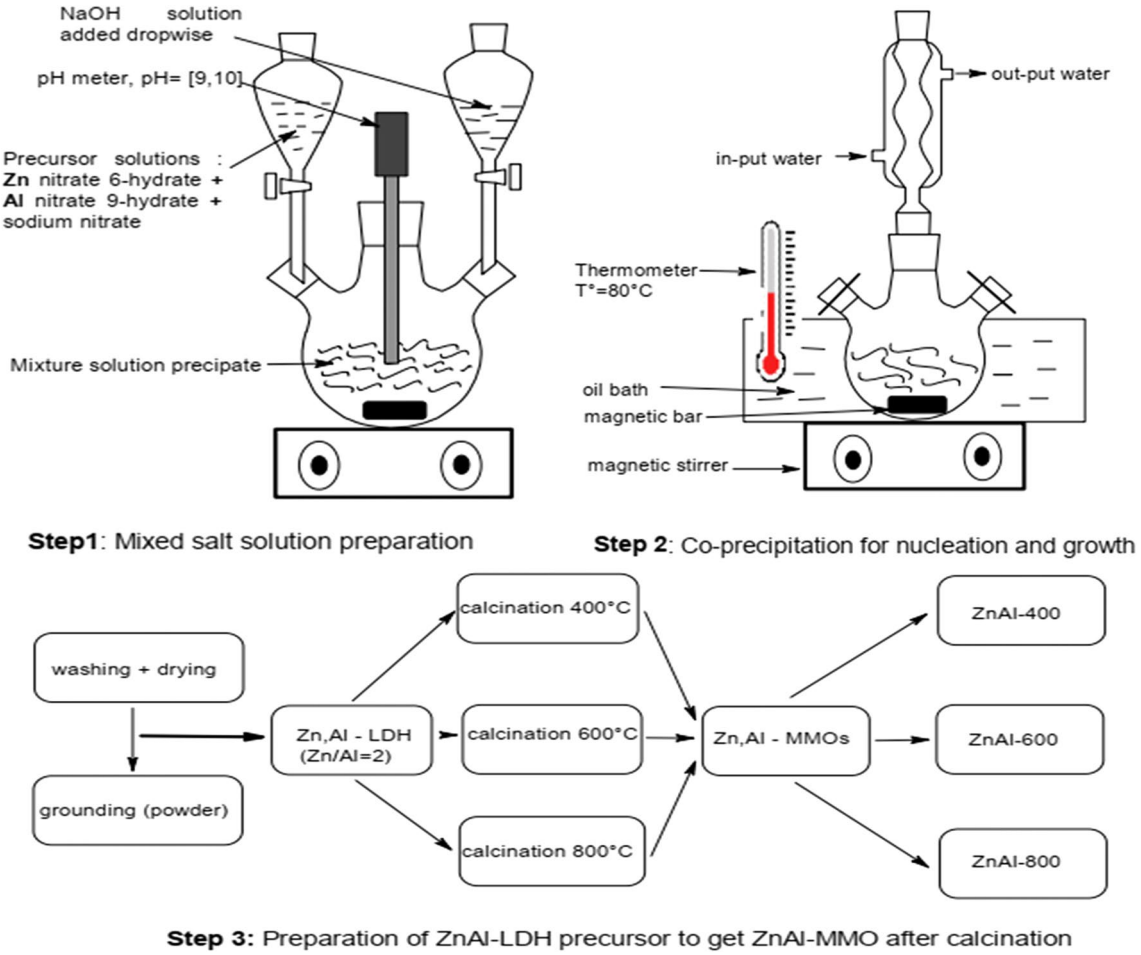

Scheme 1 Synthesis Steps of ZnAl-LDH and ZnAl-MMO Materials using the Co-Precipitation Method

powder is shown in (Fig. 1). The diffraction peaks present in the XRD diffract gram are identical to the two-phase ZnO reference pattern (PDF number 65–3411) and Zinc Aluminum Carbonate Hydroxide Hydrate (Zn0.67Al0.33 (OH) 2 (C O3)0.165·xH2 O) reference pattern (PDF number 48–1023). When the temperature of calcination was raised to 400 °C, the amount of ZnO in the phase increased from 2.7% to 21% (reference pattern, PDF number 65–3411). The second phase amount of 79% of the $ZnAl_2O_4$ appeared (reference pattern, PDF number 01–1146). At 600 °C, the XRD results indicate that the ZnO phase was present but in a lower percentage than at 400 °C (reference pattern, PDF number PDF65-3411). The $ZnAl_2O_4$ phase was also present, but at a higher percentage than at 400 °C (reference pattern, PDF number 05–0669) When the temperature of calcination was raised to 400 °C. After reaching a calcination temperature the 800 °C, the XRD spectrum obtained reveals the presence of a pure phase of Zinc Aluminum Oxide ($ZnAl_2O_4$) (reference pattern, PDF number 82–1043).

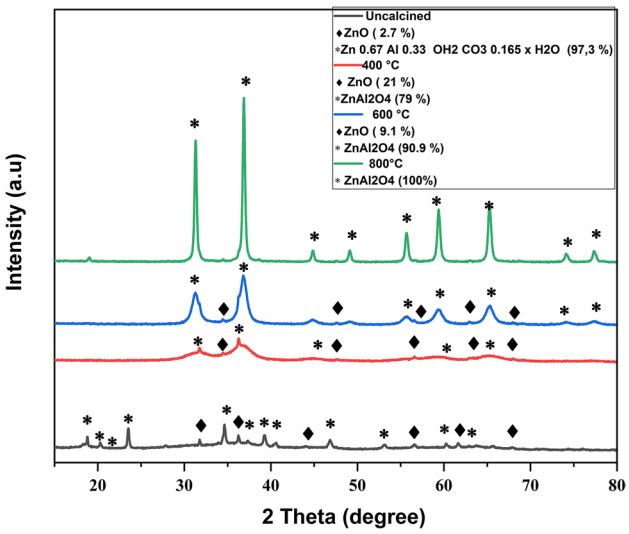

Fig. 1 XRD diffraction patterns of ZnAl-LDH and ZnAl-MMO obtained at different temperature of calcination: **a**) ZnAl-LDH; **b**) ZnAl-400; **c**) ZnAl-600; and **d**) ZnAl-800

The presence of carbonate phases in the X-ray diffraction (XRD) analysis of uncalcined ZnAl-DHD indicates contamination with carbon dioxide, which is a common issue encountered during the preparation of Layered Double Hydroxides (LDHs) using various methods, including the co-precipitation method. When LDH samples are exposed to atmospheric carbon dioxide, it can lead to the formation of carbonate anions. These carbonate anions tend to be incorporated into the interlayer of the LDH structure and tightly bound(Nyambo et al. 2008; Cardinale et al. 2023).

The mean crystallite size D of the synthesized nanoparticles was estimated using the Debye-Scherer's formula (Table 1): (Boulkroune et al. 2019; Boudiaf et al. 2021; Salima et al. 2023).

Table 1 The different parameters obtained from X-ray diffraction spectra

Samples	Grain size (nm)
Uncalcined ZnAl-LDH	34
ZnAl-400	4
ZnAl-600	8
ZnAl-800	23

$$D = \frac{0.9\lambda}{\beta \cos\theta} \quad (1)$$

where λ is the used wavelength (λ = 1.5406 Å) and Θ, the Bragg's diffraction angle.

SEM analysis

SEM was used to characterize the morphology of synthesized materials. SEM images of uncalcined ZnAl-LDH and that calcined ZnAl-MMO at different temperatures (400,600 and 800° C) are exhibited in Fig. 2a, b, c, and d, respectively (S.M). The fine, granular, and spherical shaped particles are visible in the SEM image (Fig. 2) of ZnO-$ZnAl_2O_4$. Some aggregation is also seen because particles stick together while being washed.

Optical properties

The UV–Vis absorption study of uncalcined (ZnAl-LDH) and calcined (ZnAl-MMO) at different temperatures (400, 600, and 800 °C) samples have been carried out over the wavelength range of 200 nm to 900 nm. Figure 3 shows the absorption spectra of the materials obtained at different temperatures of calcination, with the absorption peaks at 239 nm and 231 nm

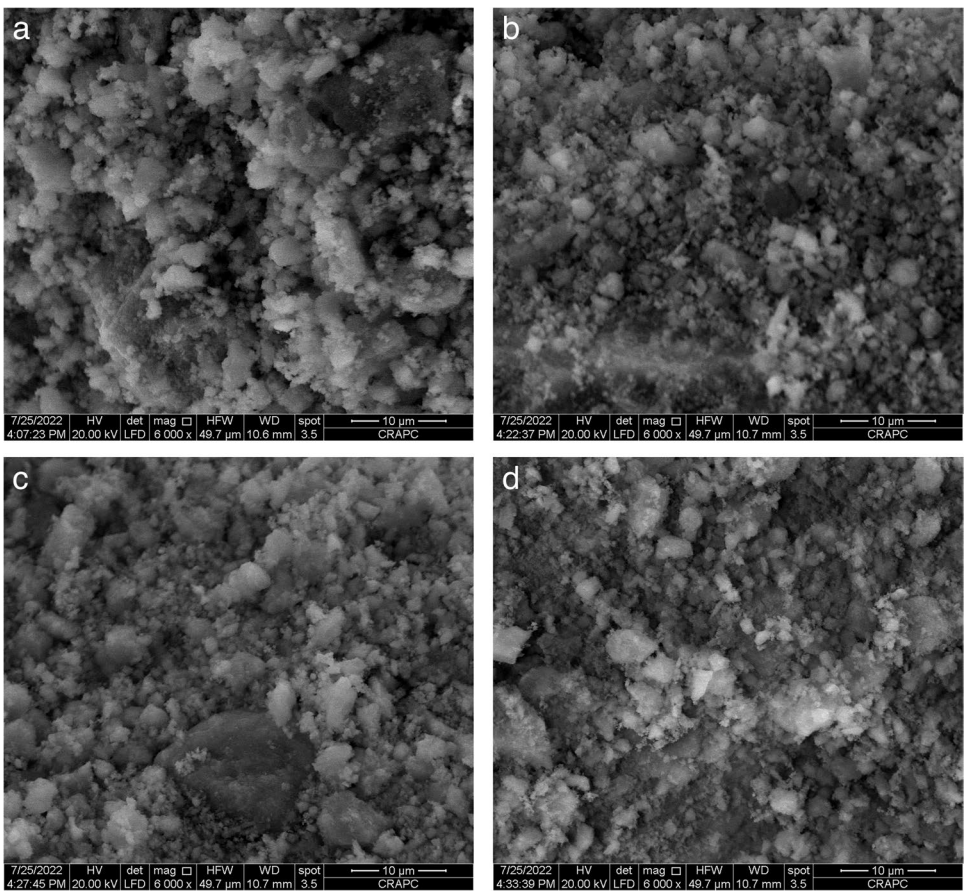

Fig. 2 SEM images of the synthesized ZnAl-LDH and ZnAl-MMO obtained at different temperature of calcination: **a**) ZnAl-LDH; **b**) ZnAl-400; **c**) ZnAl-600; and **d**) ZnAl-800

for ZnAl-LDH and ZnAl-400, respectively. Similarly, absorbance peaks like this one show the existence of the ZnO phase. The absorption peaks at 267 nm and 271 nm are for ZnAl 600 and ZnAl 800, respectively; which indicate the presence of the $ZnAl_2O_4$ phase. The absorption peak for ZnO-$ZnAl_2O_4$ (ZnAl-600) was enlarged and shifted to the longer wavelength, which indicates synergistic effects between $ZnAl_2O_4$ and ZnO.

The absorption coefficient F(R) is calculated from the reflectance curves using the Kubelka Munk equation to estimate the band gap energy *Eg*.(Bouarroudj et al. 2023, 2021; Salima et al. 2023; Tairi et al. 2022)

$$F(R) = \frac{(1-R)^2}{2R} \quad (2)$$

where R is the reflectance and F(R) is equivalent to the absorption coefficient α.

The optical band gaps (Eg) of the uncalcined ZnAl-LDH and that calcined at different temperatures ZnAl-MMO (400,600 and 800° C), were calculated using the Tauc relationship: $(\alpha hv)^2 = A\ (hv—Eg)$.The extrapolation of the linear part of Tauc plots intersects with the photon energy axis to define Eg,shown in Fig. 4a, b, c, and d, respectively (S.M). The band gap of ZnAl-LDH nanoparticles was determined to be 3.8 eV, while for ZnAl-400; the band energy was measured at 3.52 eV and 4.14 eV relative to two materials confirmed by XRD. Additionally, the band gap for ZnAl-600 and ZnAl-800 was found to be 3.7 eV and 3.8 respectively.

FTIR characterization

The FTIR spectrum of ZnAl-LDH and ZnAl-MMO (ZnO-$ZnAl_2O_4$) is presented in Fig. 5. The infrared spectra (FTIR) of the material were between 400 and 4000 cm^{-1}, which shows the chemical bonds and functional groups in the compound. The significant absorption band centered at 3396 cm^{-1} is caused by the O–H stretching vibration of water molecules on the surface and in the spaces between the layers of the material(Nickel and Fleischer 2003; Iaiche and Djelloul 2015; Ghribi et al. 2020). The band at 1640 cm^{-1} is caused by the water molecule's H–O-H scissor-bending vibration. The strong and distinct band at 1357 cm-1 is attributed to the presence of nitrate ions (Wang et al. 2015; Touahra et al. 2016; Iaiche et al. 2020). The bands at 3396 cm^{-1}, 1640 cm^{-1} and 1357 cm^{-1}in ZnAl-LDH are not present in the corresponding calcined samples at 600 and 800°C, which are attributed to the removal of water molecules and the decomposition of the NO^{3-}groups in the LDH interlayer. The absorption peak located at 423 cm^{-1}, corresponding to the Zn–O vibration frequency(Bouzid et al. 2009; Iaiche and Djelloul 2015). The two peaks at 518 and 650 cm^{-1} are caused by Al-O stretching and O–Al-O bending vibrations of the AlO_6 group in the spinel-type $ZnAl_2O_4$ structure, respectively(Abd El All et al. 2007; Sunder et al. 2011; Abd-Allah et al. 2022). The FT-IR and XRD results are in good agreement to confirm ZnO and $ZnAl_2O_4$ as mixed metal oxides formation.

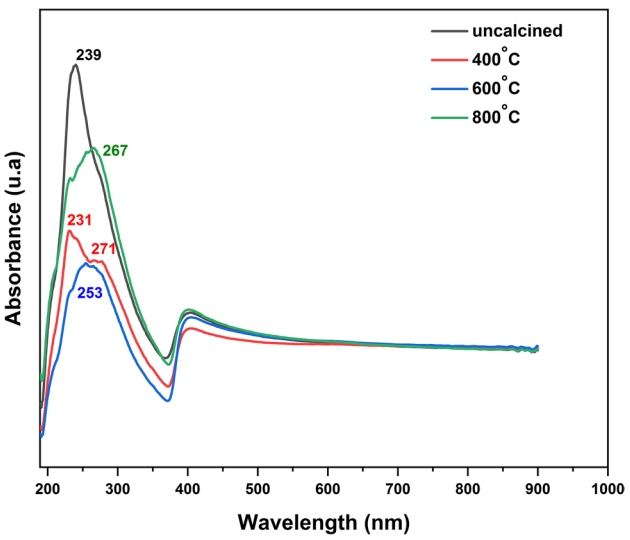

Fig. 3 UV–Vis spectra of ZnAl-LDH, ZnAl-400, ZnAl-600, and ZnAl-800 obtained at different temperature of calcination

Antibacterial activity

Effects of ZnO-$ZnAl_2O_4$ on Gram-Positive Bacteria

Effects on Gram-Positive Cocci Figure 6 (a,b) displays the results of the minimum inhibitory concentration (MIC) and minimum bactericidal concentration (MBC) tests conducted at different temperatures (400, 600, and 800 °C). Remarkably, the Staphylococcus aureus ATCC43300 strain exhibited a MIC of 0.5 µg/mL when treated with ZnAl 800, indicating a strong inhibitory effect. Additionally, the Enterococcus faecalis ATCC29212 strain demonstrated a MIC of 0.25 µg/mL when exposed to the uncalcined material, suggesting its potential as an effective antimicrobial agent. Notably, all other Gram-positive cocci strains showed a MIC of 0.125 µg/mL, signifying a consistent antimicrobial response. The MBC values ranged from 0.250 to 16 µg/mL, with ZnAl 400 and ZnAl-600 respectively, highlighting the varying bactericidal effects of the different materials and temperatures used in the study. These results confirm the conclusion that Zn^{2+}, released from ZnO particles interacting with the bacterial medium, can exhibit significant antimicrobial activity against Gram-positive bacteria, particularly cocci(Pasquet et al. 2014; Cardinale et al. 2023). Figure 6 (b) (S.M).

Table 2 presents the compiled results of the ratio (MBC/MIC) obtained from treating gram-positive cocci bacteria with varying concentrations of uncalcined ZnAl-LDH and calcined ZnAl-MMO at three different temperatures

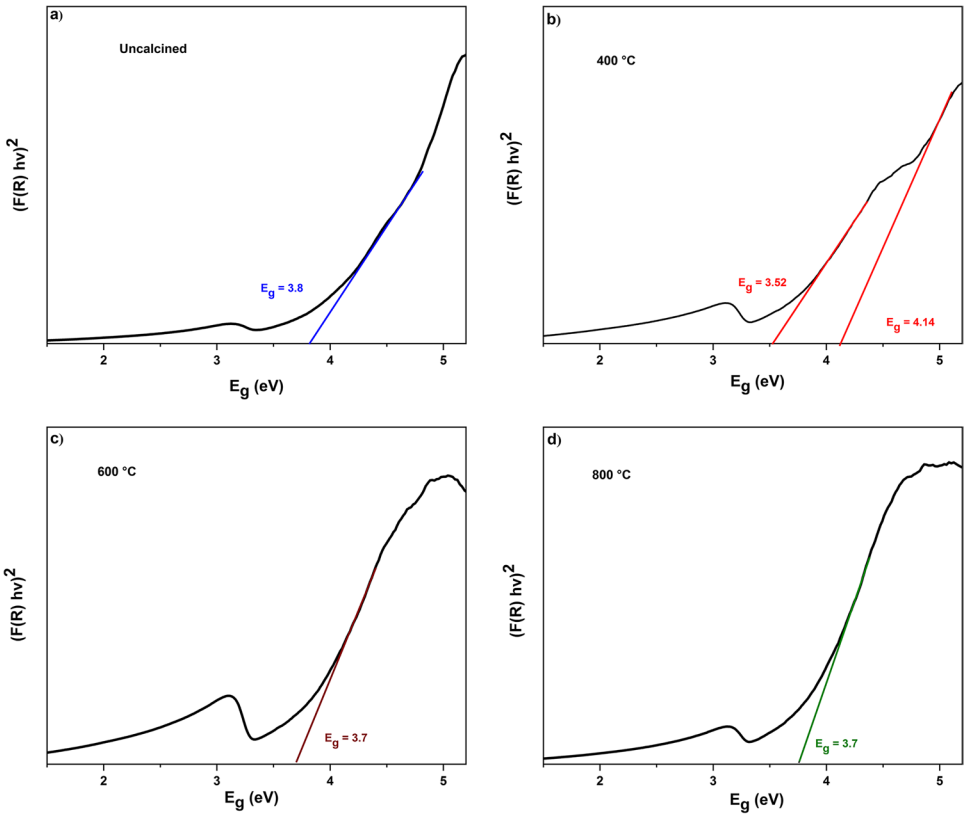

Fig. 4 UV–Vis absorption data fitted by Tauc's formula for direct band gap: **a** ZnAl-LDH; **b** ZnAl-400; **c** ZnAl-600; and (**d**) ZnAl-800

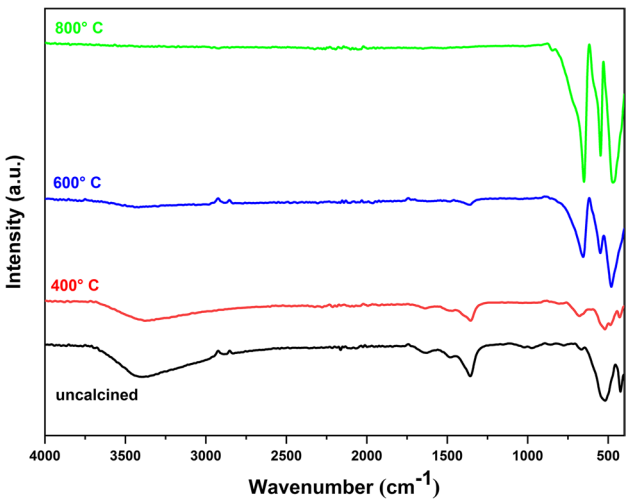

Fig. 5 FT-IR spectra of ZnAl-LDH and ZnAl-MMO obtained at different temperature of calcinations

(400 °C, 600 °C, and 800 °C). Our findings demonstrate that the uncalcined material possesses bactericidal properties against all three strains: S. aureus 43300, S. aureus cipro. R, and E. faecalis ATCC 29212. However, the material calcined at temperatures of 400 °C, 600 °C, and 800 °C exhibits its bacteriostatic characteristics specifically against the S. aureus cipro. R strain. Notably, when treated with ZnAl-600, the material demonstrates a tolerant nature towards certain strains of the Staphylococcus genus.

Effects on Gram-Positive Bacillus Figure 7(a,b) presents the MIC and MBC values obtained when treating Gram-positive bacillus bacteria with varying concentrations of ZnAl-LDH and ZnAl-MMO calcined at different temperatures (400, 600, and 800 °C). Analyzing the results of the treatment on Gram-positive bacillus, it is observed that the Bacillus cereus strain exhibited a MIC of 1 µg/mL when exposed to ZnAl-800 material, while a MIC of 0.125 µg/mL was obtained with the other tested materials. Bacillus 16404 displayed a MIC of 0.125 µg/mL for all calcined materials. Furthermore, the MBC for the Bacillus genus strain ranged from 0.25 to 32 µg/mL with different ZnAl-MMO samples. These findings align with the work of Lin et al. (2009), who investigated ZnO-Al_2O_3 composites with various Zn/Al molar ratios (2, 2.5, 3, 3.5, and 4). Through calcination of ZnRAl-CO_3-HDLs at 500 °C using a nucleation and aging method (SNAS), they evaluated the efficacy against Staphylococcus aureus ATCC 6538. Their results demonstrated that ZnO-$ZnAl_2O_4$ composites effectively eliminated Staphylococcus aureus ATCC 6538, Bacillus subtilis var, and Bacillus subtilis var Niger ATCC 9372, including their spores. The effectiveness of killing Bacillus subtilis var Niger ATCC 9372 increased with ZnO content due to the heterojunction

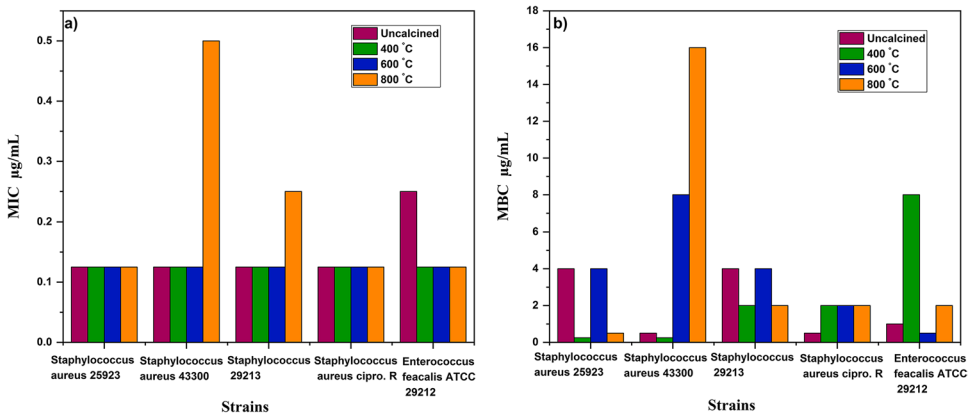

Fig. 6 **a** Values of MIC of Gram-positive cocci treated with ZnAl-LDH, ZnAl-400, ZnAl-600, and ZnAl-800, **b** Values of MBC of Gram-positive cocci treated with ZnAl-LDH, ZnAl-400, ZnAl-600, and ZnAl-800

Table 2 Values of the ratio (MBC/MIC) of Gram-positive cocci treated with ZnAl-LDH, ZnAl-400, ZnAl-600, and ZnAl-800

Ratio of MBC/MIC					
Temperature of calcination	*S. aureus* 25,923	*S.aureus*43300	S.29213	*S. aureus* cipro. R	*E. feacalis* ATCC 29212
Uncalcined ZnAl LDH	32	4	32	4	4
ZnAl 400° C	2	2	16	16	64
ZnAl 600° C	32	64	32	16	4
ZnAl 800° C	4	32	8	16	16

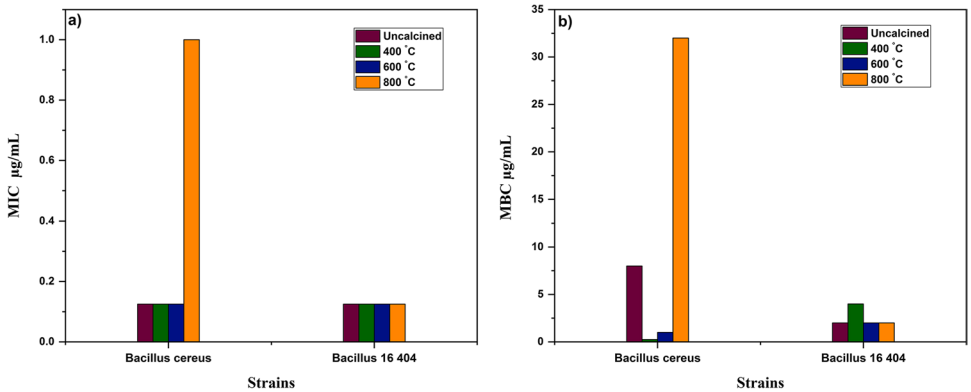

Fig. 7 **a** Values of MIC of Gram-positive bacillus treated with ZnAl-LDH, ZnAl-400, ZnAl-600, and ZnAl-800, **b** Values of MBC of Gram-positive bacillus treated with ZnAl-LDH, ZnAl-400, ZnAl-600, and ZnAl-800

structure of ZnO-Al_2O_3 composites. The presence of ZnO in the composites led to the generation of O_2^- and ^-OH, which interacted with the -NH-CO- bonds, resulting in the breakdown of bacterial walls, apoptosis, and cell death (Lin et al. 2009). Figure 7(b) (S.M).

Table 3 provides a summary of the ratio (MBC/MIC) values obtained from treating gram-positive bacillus bacteria with different concentrations of uncalcined ZnAl-LDH and calcined ZnAl-MMO at three temperatures (400 °C, 600 °C, and 800 °C). Analyzing the results of the treatment on gram-positive bacilli, it is evident that both ZnAl-LDH in its uncalcined form and the calcined ZnAl-MMO materials exhibit bacteriostatic properties when tested against the Bacillus 16404 strain. However, interestingly, the same strain shows tolerance towards ZnAl-400. On the other hand, the Bacillus cereus strain demonstrates tolerance towards both ZnAl-LDH and ZnAl-MMO at 800 °C. The desired bactericidal effect is achieved with ZnAl-MMO at 400 °C.

Effect of ZnAl-LDH and ZnAl-MMO on Gram-negative bacteria

Effect on Lactose positive Enterobacteriaceae Figure 8 (a, b) presents the MIC and MBC values obtained from treating Lactose positive Enterobacteriaceae with varying concentrations of ZnAl-LDH, ZnAl-400, ZnAl-600, and ZnAl-800. It is observed that with ZnAl-LDH, ZnAl-400, and ZnAl-600, the MIC for lactose-positive Enterobacteriaceae is approximately 0.125 µg/mL However, when using ZnAl-800, the

Table 3 Values of the ratio (MBC/MIC) of Gram-positive bacillus treated with ZnAl-LDH, ZnAl-400, ZnAl-600, and ZnAl-800

Ratio of MBC/MIC		
Temperature of calcination	*Bacillus cereus*	*Bacillus 16,404*
Uncalcined ZnAl LDH	64	16
ZnAl 400° C	2	32
ZnAl 600° C	8	16
ZnAl 800° C	32	16

Table 4 Values of the ratio (MBC/MIC) of lactose-positive Enterobacteriaceae treated with ZnAl-LDH, ZnAl-400, ZnAl-600, and ZnAl-800

Ratio of MBC/MIC					
Temperature of calcination	*E. coli B.L.S.E*	*E. coli M.C.R.1*	*Klebsiella oxytoca*	Kpc-	Kpc +
Uncalcined ZnAl LDH	8	4	4	4	8
ZnAl 400° C	8	64	8	4	32
ZnAl 600° C	4	64	4	4	2
ZnAl 800° C	4	16	128	8	4

MIC ranges from 0.125 to 2 µg/mL as for the MBC; it varies within the range of 0.5 to 16 µg/mL, depending on the specific ZnAl-MMO material used.

Nanoparticles have shown promising activity against lactose-positive Enterobacteriaceae bacteria. Nanoparticles have the ability to disrupt bacterial cell membranes, leading to leakage of essential components and disruption of vital processes. Additionally, nanoparticles can induce oxidative damage at the cellular level, resulting in deterioration of bacterial DNA and proteins(Juan et al. 2021). Figure 8 (b)(S.M).

Table 4 compiles the ratio (MBC/MIC) values obtained after treating lactose-positive Enterobacteriaceae with different concentrations of ZnAl-LDH, ZnAl-400, ZnAl-600, and ZnAl-800. It is noteworthy that ZnAl-LDH demonstrates bactericidal activity against strains of E. coli M.C.R.1, Klebsiella oxytoca, and Kpc-. Similarly, ZnAl-600 exhibits bactericidal effects against E. coli B.L.S.E., Klebsiella oxytoca, Kpc-, and Kpc + strains. However, strains of E. coli M.C.R.1 and Kpc + display tolerance towards ZnAl-400 treatment. Additionally, E. coli M.C.R.1 and Klebsiella oxytoca strains demonstrate tolerance towards ZnAl-400 and ZnAl-800 materials, respectively.

Effect on Lactose negative Enterobacteriaceae Figure 9 (a,b) presents the MIC and MBC values obtained when treating lactose-negative Enterobacteriaceae with varying concentrations of ZnAl-LDH and ZnAl-MMO calcined at different temperatures (400, 600, and 800 °C). Notably, the strain Salmonella typhi 14028 exhibited an MIC of 0.125 µg/mL The CMB values were 0.250 µg/mL for ZnAl-400 and ZnAl-600, and 1 µg/mL for ZnAl-LDH. It is worth mentioning that the CMB for ZnAl-800 was 8 µg/ mL.The presence of prepared nanoparticles (NPs) in the bacterial medium triggers the secretion of reactive oxygen species (ROS). These ROS play a crucial role in facilitating the penetration of NPs through the bacterial cell membrane and subsequently inactivating the bacteria. The bactericidal activity of NPs becomes more pronounced as the concentration of NPs increases(Meena Kumari and Philip 2015; Vidhu and Philip 2015). Figure 9 (b) (S.M).

Table 5 presents the ratios (MBC/MIC) obtained when treating lactose-negative Enterobacteriaceae with different concentrations of uncalcined ZnAl-LDH and calcined ZnAl-MMO at temperatures of 400°c, 600°c, and 800°c. The results indicate that the uncalcined material ZnAl-LDH demonstrated bacteriostatic properties against salmonella typhi 14028, while the same bacterial strain exhibited bactericidal properties when treated with ZnAl-400 and ZnAl-600.

Effects on Gram-negative bacillus

Figure 10(a, b, c, d) presents the MIC and MBC values obtained when treating Gram-negative bacilli with varying

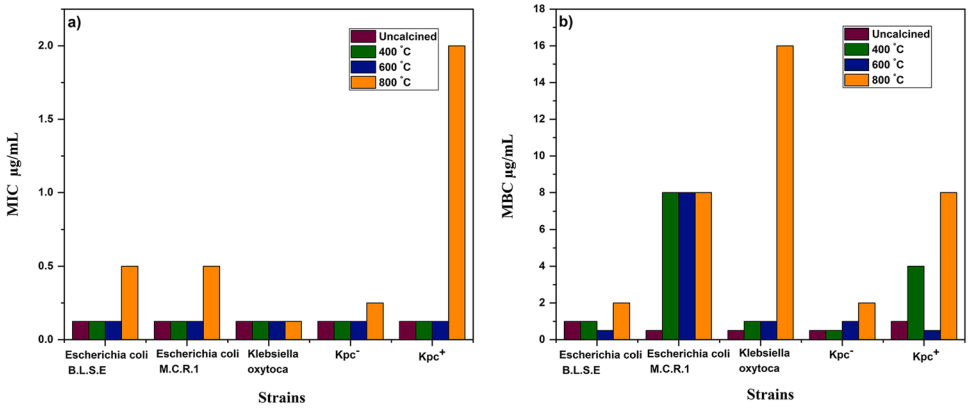

Fig. 8 **a** Values of MIC of Lactose positive Enterobacteriaceae treated with ZnAl-LDH, ZnAl-400, ZnAl-600 and ZnAl-800, **b** Values of MBC of Lactose positive Enterobacteriaceae treated with ZnAl-LDH, ZnAl-400, ZnAl-600 and ZnAl-800

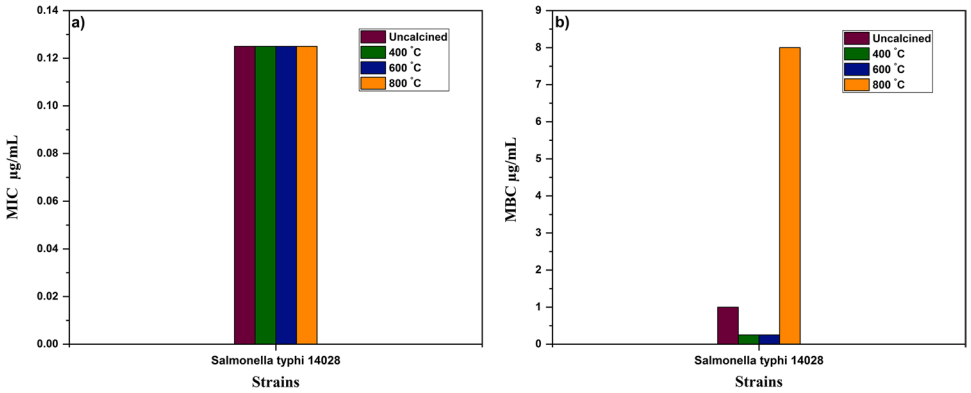

Fig. 9 **a** Values of MIC of Lactose negative Enterobacteriaceae treated with ZnAl-LDH, ZnAl-400, ZnAl-600, and ZnAl-800. **b** Values of MBC of Lactose negative Enterobacteriaceae treated with ZnAl-LDH, ZnAl-400, ZnAl-600, and ZnAl-800

Table 5 Values of the ratio (MBC/MIC) of lactose-negative Enterobacteriaceae treated with ZnAl-LDH, ZnAl-400, ZnAl-600, and ZnAl-800

Ratio of MBC/MIC	
Temperature of calcination	*Salmonella typhi 14028*
Uncalcined ZnAl LDH	8
ZnAl 400° C	2
ZnAl 600° C	2
ZnAl 800° C	64

concentrations of ZnAl-LDH and ZnAl-MMO. The results obtained for the GNB strains indicate that Acinetobacter baumannii MDR 05, Elizabethkingia anophelis, and Sphingomonas paucimobilis exhibited MIC values ranging from 0.250 to 2 µg/mL for ZnAl-800, while the Acinetobacter OXA23 strain displayed an MIC of 0.25 µg/mL for ZnAl-LDH material. The other strains showed an MIC of 0.125 µg/mL across different calcination temperatures. The CMB values ranged from 0.250 to 8 µg/mL for various ZnAl-MMO materials. In a study by Suprabha Yadav et al. (2020) it was reported that ZnO/Al_2O_3 (ZANC) nanocomposites synthesized with different Zn: Al ratios and calcined at temperatures ranging from 400 °C to 1000 °C exhibited inhibition efficiencies of 86.86%, 87.29%, and 100% against strains of S. aureus, P. aeruginosa, and B. subtilis, respectively (Yadav et al. 2020). These results align with our findings. Figure 10(b,d)(S.M).

Table 6 presents the results of the (MBC/MIC) ratio obtained when treating Gram-negative bacillus bacteria with ZnAl-LDH and ZnAl-MMO materials. The results obtained for the GNB strains indicate that ZnAl-LDH, ZnAl-400, ZnAl-600, and ZnAl-800 materials exhibit bactericidal properties against the S. paucimobilis strain. However, strains such as P. aeruginosa ATCC 27853, P. VIM 2, A. OXA 23, A. NDM, A. baumannii MDR 05, and S. marcescens demonstrate bacteriostatic properties when treated with ZnAl-600. Interestingly, the A. OXA 23 strain appears to have some level of tolerance to treatment with the ZnAl-800 material (Table 6).

Effect of ZnAl-LDH and ZnAl-MMO on fungi

Figure 11(a,b) displays the MIC and MBC values obtained when treating yeasts with different concentrations of ZnAl-LDH and ZnAl-MMO. Our findings reveal that the Candida albicans strain exhibited an MIC of 0.125 µg/mL across various materials. The MBC values ranged from 0.250 to 4 µg/mL to the best of our knowledge, we have not come across any published research on the effects of our ZnAl-LDH, ZnAl-400, ZnAl-600, and ZnAl-800 materials on fungi. Therefore, our results are encouraging and validate the antifungal efficacy of the tested materials against Candida albicans strains(Ayanwale et al. 2021; Djearamane et al. 2022; Arsène et al. 2023). Figure 11(b) (S.M).

Table 7 presents the values of the (MBC/MIC) ratio obtained when treating fungi with different concentrations of ZnAl-LDH, ZnAl-400, ZnAl-600, and ZnAl-800. Our findings indicate that our materials exhibit bactericidal properties against the Candida albicans strain.

Mechanisms of antimicrobial activity

Currently, there are ongoing discussions regarding the mechanism by which nanoparticles exhibit antibacterial activity. Existing scientific literature suggests that nanoparticles have the potential to inhibit the growth of various microorganisms, including bacteria and fungi. Several studies (Applerot et al. 2012; Guo et al. 2015; Suresh et al. 2016), frequently mention the generation of reactive oxygen species (ROS) by metal oxide nanoparticles as a prominent mechanism contributing to their antimicrobial effects. However, the generation of ROS appears to be somewhat perplexing, as many studies have demonstrated that it occurs under light exposure. Conversely, other studies (Adams et al. 2006;

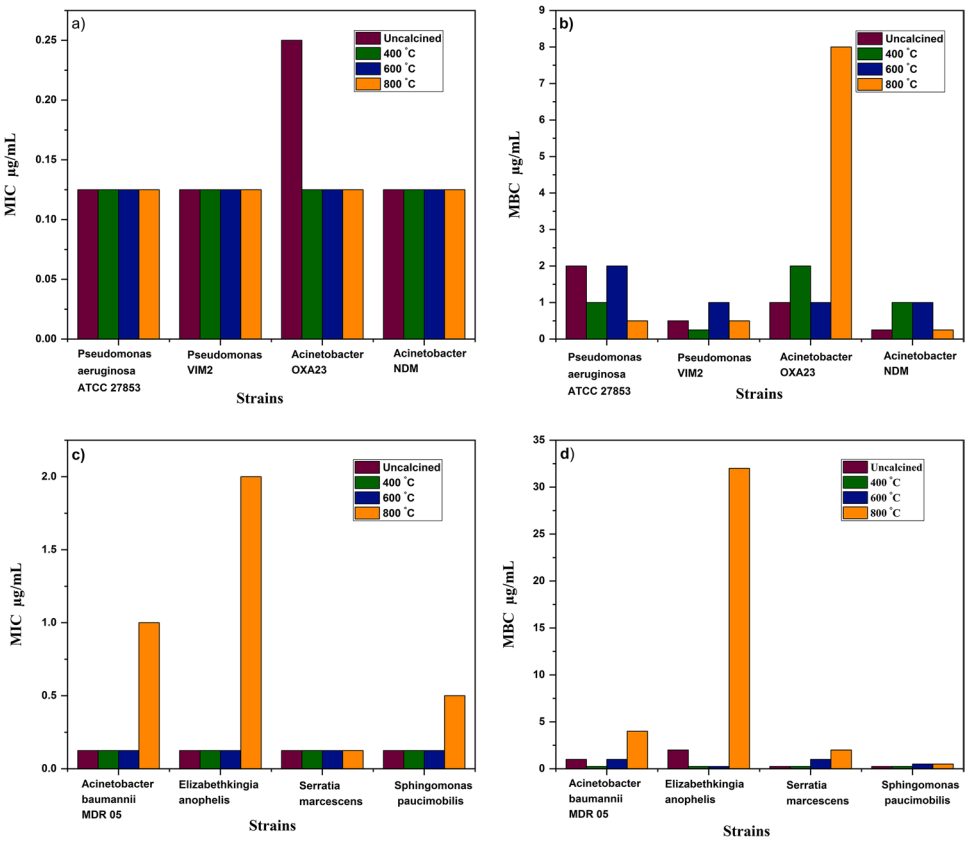

Fig. 10 **a** Values of MIC of Gram-negative bacillus treated with ZnAl-LDH, ZnAl-400, ZnAl-600, and ZnAl-800, **b** Values of MBC of Gram-negative bacillus treated with ZnAl-LDH, ZnAl-400, ZnAl-600, and ZnAl-800, **c** Values of MIC of Gram-negative bacillus treated with ZnAl-LDH, ZnAl-400, ZnAl-600, and ZnAl-800, **d** Values of MBC of Gram-negative bacillus treated with ZnAl-LDH, ZnAl-400, ZnAl-600, and ZnAl-800

Table 6 Values of the ratio (MBC/MIC) of Gram-negative bacillus treated with ZnAl-LDH, ZnAl-400, ZnAl-600, and ZnAl-800

Ratio of MBC/MIC								
Temperature of calcination	*P. aeruginosa ATCC 27853*	*P VIM 2*	*A OXA 23*	*A NDM*	*A baumannii MDR 05*	*E anophelis*	*S marcescens*	*S. paucimobilis*
Uncalcined ZnAl LDH	16	4	4	2	8	16	2	2
ZnAl 400° C	8	2	16	8	2	2	2	2
ZnAl 600° C	16	8	8	8	8	2	8	4
ZnAl 800° C	4	4	64	2	4	16	16	2

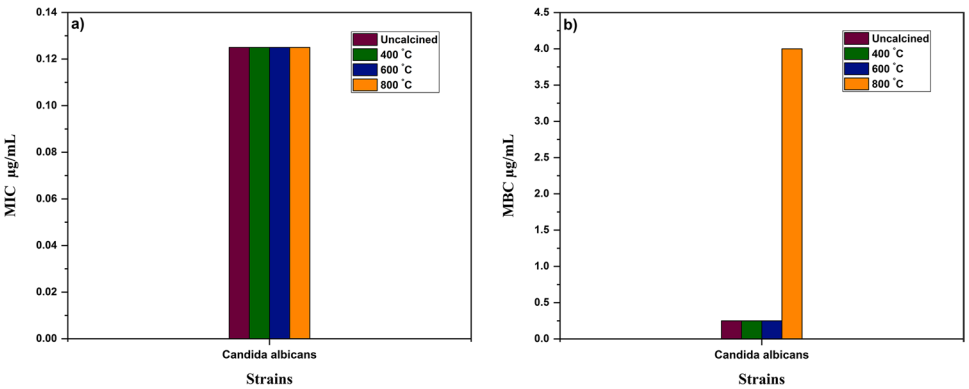

Fig. 11 **a** Values of: MIC of fungi treated with ZnAl-LDH, ZnAl-400, ZnAl-600, and ZnAl-800, **b** Values of: MBC of fungi treated with ZnAl-LDH, ZnAl-400, ZnAl-600, and ZnAl-800

Table 7 Values of the ratio (MBC/MIC) of fungi treated with ZnAl-LDH, ZnAl-400, ZnAl-600 and ZnAl-800

Ratio of MBC/MIC	
Temperature of calcination	*Candida albicans*
Uncalcined ZnAl LDH	2
ZnAl 400° C	2
ZnAl 600° C	2
ZnAl 800° C	32

Hirota et al. 2010; Sirelkhatim et al. 2015) have reported that this activity also occurs in the absence of light, suggesting an alternative explanation. (Hirota et al. 2010) conducted experiments using ZnO-NPs against E. coli and observed the generation of reactive oxygen species (ROS) even in the absence of light. This finding was consistent with the results reported by (Jones et al. 2008), which also indicated the production of superoxide species. These consistent findings suggest the existence of unidentified processes that may be responsible for the generation of reactive species in the absence of light.

According to researchers, in the absence of light or under visible light with photon energy lower than the ZnO band gap, the sources of electrons and holes that contribute to antibacterial activity are electronic defects. These defects include the negatively charged Zni defect for electrons and the positively charged Zinc vacancy Vzn defect for holes. Studies on photoluminescence (PL) have revealed that the presence of these two defects increases with In doping (Danial et al. 2020). This suggests that the Zni and Vzn defects play a crucial role in the production of reactive oxygen species (ROS) that are responsible for inhibiting bacterial growth (Ravichandran et al. 2015; Vijayaprasath et al. 2016; Zhang et al. 2017; Danial et al. 2020).

Oxidative stress is a chemical mechanism that plays a significant role in the activity of bactericides. It refers to an imbalance between the excessive formations of reactive oxygen species (ROS) and the antioxidant defense system. ROS are highly reactive compounds derived from oxygen, including singlet oxygen ($^1O_2$), superoxide ($^{\bullet}O^-_2$), hydroxyl ions (OH), hydroxyl radicals ($^{\bullet}OH$), and peroxides (H_2O_2). These ROS can cause oxidative damage to lipids, proteins, and DNA, which can be detrimental to cellular health. When present in high concentrations, ROS can be extremely harmful to organisms, leading to lipid peroxidation, protein oxidation, DNA damage, enzyme inhibition, activation of the programmed cell death (PCD) pathway, and ultimately, cell death.(Hancock et al. 2001; Díez-Pascual and Luceño-Sánchez 2021).

Another mechanism that has been investigated involves the release of zinc ions (Zn2+) resulting from the dissolution of ZnO nanoparticles (NPs) (Li et al. 2011; Pasquet et al. 2015). The presence of zinc can interfere with the enzymatic system, leading to a slowdown in the metabolism of amino acids (Sirelkhatim et al. 2015).

The adsorption of nanoparticles (NPs) onto bacterial membranes is an inherent toxicological phenomenon. The physical chemistry of the surrounding environment plays a role in determining the extent of adsorption and subsequent deleterious effects. The presence of NPs destabilizes the membrane, leading to the leakage of water and intracellular ions. As a result, the membrane loses its semi-permeable barrier function. This disruption creates significant osmotic stress at the cellular level, ultimately resulting in cell death (Mager et al. 2000; Gunasekera et al. 2008). The scientific literature suggests that the attraction between bacteria and metal oxide NPs is mediated by electrostatic forces. According to the hypothesis proposed by Stoimenov et al. (2002), metallic oxide nanoparticles adhere to bacteria electrostatically, leading to the rupture of the bacterial cell membrane and subsequent bacterial death (Stoimenov et al. 2002).

Mechanism of ROS production

The presence of oxygen vacancies enhances the acidic nature of the surface, thereby increasing the attractive interaction with H_2O (Lewis base). When water molecules occupy these electrophilic sites, hydroxyl groups (OH^-) are formed. Indeed, oxygen vacancies have the ability to dissociate H_2O by transferring a proton to a neighboring oxygen atom, thus forming two hydroxyl groups for each vacancy. This dissociation allows the hydroxyl groups to form hydrogen bonds with neighboring water molecules. Thus, the presence of oxygen vacancies promotes the formation of hydroxyl groups and strengthens the interactions between the surface and water molecules. However, it is worth noting that these hydroxyl radicals can also play a role in bacterial cell death, as they can cause oxidative damage to membranes and DNA, thereby inhibiting bacterial growth Scheme 2 (S.M). (Ravichandran et al. 2015; Mrabet et al. 2016; Biswas et al. 2022; Querebillo 2023).

We propose the following mechanism for the production of ROS in the dark (Narayana et al. 1982; Lupan et al. 2009; Lakshmi Prasanna and Vijayaraghavan 2015):

$$O_2 + e^- \rightarrow^{\bullet} O - 3 \quad (3)$$

$$^{\bullet}O^-_2 + H_2O \rightarrow^{\bullet} HO_2 + OH^4 \quad (4)$$

$$^{\bullet}HO_2 +^{\bullet} HO_2 \rightarrow H_2O_2 \quad (5)$$

Scheme 2 Mechanism of ROS production via oxygen vacancies

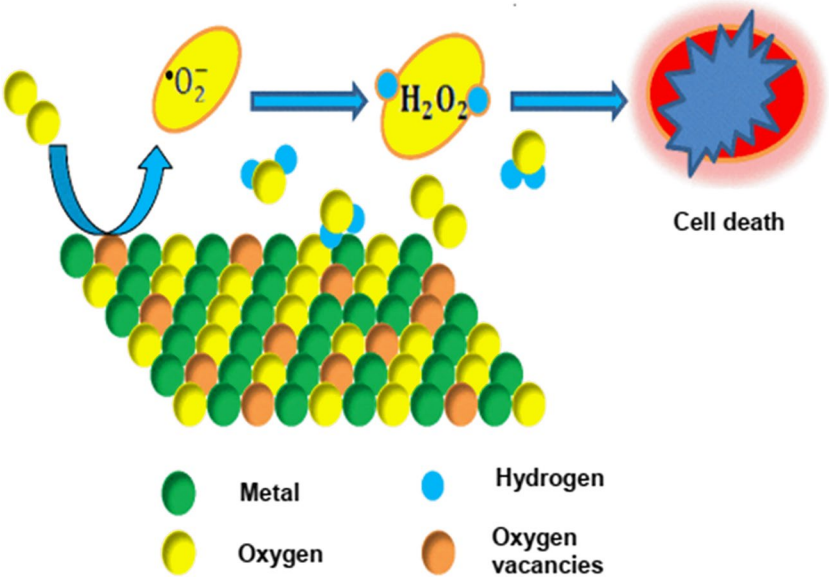

$$H_2O_2 + {}^{\bullet}O^-{}_2 \rightarrow O_2 + {}^{\bullet}OH + OH^- \quad (6)$$

Antibacterial mechanism of prepared nanomaterials

(1) ZnO-$ZnAl_2O_4$ nanomaterials disrupt cell walls and cytoplasmic membranes by releasing ions that adhere to or pass through them. (2) These ions denature ribosomes and inhibit protein synthesis. Additionally, they deactivate the respiratory enzyme on the cytoplasmic membrane, (3) leading to the interruption of adenosine triphosphate (ATP) production. (4) Reactive oxygen species produced by the damaged electron transport chain can also cause membrane disruption. (5) ZnO-$ZnAl_2O_4$ nanomaterials, along with reactive oxygen species, bind to deoxyribonucleic acid (DNA) and prevent its replication and cell multiplication. (6) By accumulating in the pits of the cell wall, these nanoparticles also denature the membrane. (7) Furthermore, ZnO-$ZnAl_2O_4$ nanomaterials can directly traverse the cytoplasmic membrane, potentially resulting in the release of cell organelles Scheme 3 (S.M) (You et al. 2012; Slavin et al. 2017; Gupta and Bahadur 2018; Yin et al. 2020; Yu et al. 2020).

Scheme 3 Antibacterial mechanism of prepared nanomaterials

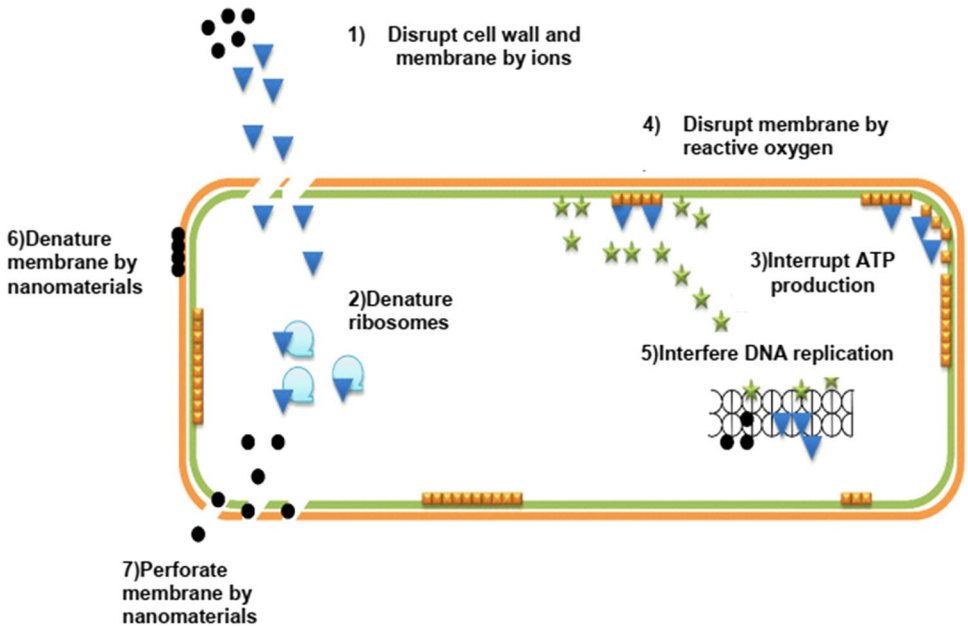

Conclusion

ZnAl-LDH was synthesized using the co-precipitation method, followed by calcination at different temperatures (400, 600, and 800°C) to obtain ZnAl mixed metal oxides. Characterization results revealed the formation of ZnO-$ZnAl_2O_4$ at a calcination temperature of 400 and 600°C, while $ZnAl_2O_4$ as spinel was obtained at 800°C.

In this study, we conducted an in vitro evaluation of the antimicrobial activity of ZnAl-LDH, ZnAl-400, ZnAl-600, and ZnAl 800 against a panel of 21 bacterial strains, including 15 clinical strains, 6 Gram-reference strains, and one fungal strain. Our findings demonstrated that ZnAl-LDH, ZnAl- 400, and ZnAl-600 exhibited minimum inhibitory concentration (MIC) values of 0.125 µg/mL against the tested strains. MIC values ranging between 0.125 and 2 µg/mL were obtained with ZnAl-800, and it was observed that Enterobacteriaceae and non-Enterobacteriaceae bacteria were more susceptible compared to Gram-positive bacteria. Thus, ZnAl-LDH and ZnAl-MMO showed greater effectiveness against gram-positive bacteria than gram-negative bacteria, possibly attributed to the formation of a type II heterojunction structure between ZnO and $ZnAl_2O_4$, which occurs at 400 and 600°C.

In conclusion, the mixed metal oxides (ZnO-$ZnAl_2O_4$) derived from the calcination of ZnAl-LDH, synthesized via the co-precipitation method, show promising potential as alternatives to antibiotics. These mixed metal oxides could be employed as an impregnating agent in a matrix to prevent microbial contamination by inhibiting microorganisms that come into contact with or approach the receptive surface.

Author contribution Each author participated sufficiently in the work. AD, ZB and KB supervision; FG, TB, YM, I B, AC, BA, BA, HB, and OLconceptualization, methodology, writing—original draft preparation, formal analysis and investigation, writing—review and editing. All authors reviewed the manuscript.

Funding Not applicable.

Data availability All data and materials used in this study are available within this article.

Declarations

Ethical approval Not applicable.

Competing interests The authors declare no competing interests.

References

Abd El All S, Fawzy YHA, Radwan RM (2007) Study on the structure and electrical behaviour of zinc aluminate ceramics irradiated with gamma radiation. J Phys D Appl Phys 40:5707–5713. https://doi.org/10.1088/0022-3727/40/18/029

Abd-Allah A, Amin A, Youssef A, Ahmed Y (2022) Fabrication of zinc aluminate (ZnAl2O4) nanoparticles from solid industrial wastes. Egypt J Pure Appl Sci 60:14–26. https://doi.org/10.21608/ejaps.2022.132250.1032

Adams LK, Lyon DY, Alvarez PJJ (2006) Comparative eco-toxicity of nanoscale TiO2, SiO2, and ZnO water suspensions. Water Res 40:3527–3532. https://doi.org/10.1016/j.watres.2006.08.004

Applerot G, Lellouche J, Perkas N et al (2012) ZnO nanoparticle-coated surfaces inhibit bacterial biofilm formation and increase antibiotic susceptibility. RSC Adv 2:2314–2321. https://doi.org/10.1039/c2ra00602b

Arsène MMJ, Viktorovna PI, Alla M et al (2023) Antifungal activity of silver nanoparticles prepared using Aloe vera extract against Candida albicans. Vet World 16(1):18. https://doi.org/10.14202/vetworld.2023.18-26

Ayanwale AP, Estrada-Capetillo BL, Reyes-López SY (2021) Evaluation of Antifungal Activity by Mixed Oxide Metallic Nanocomposite against Candida spp. Processes 9:773. https://doi.org/10.3390/pr9050773

Bayahia H, Mutlaq Al Ghamdi MS, Hassan MS, Amna T (2017) Facile Synthesis of ZnO-Cu2O Composite Nanoparticles and Effect of Cu2O Doping in ZnO on Antimicrobial Activity. Mod Chem Appl 05:2–5. https://doi.org/10.4172/2329-6798.1000237

Biswas A, Kar U, Jana NR (2022) Cytotoxicity of ZnO nanoparticles under dark conditions *via* oxygen vacancy dependent reactive oxygen species generation. Phys Chem Chem Phys 24:13965–13975. https://doi.org/10.1039/D2CP00301E

Bouarroudj T, Aoudjit L, Djahida L et al (2021) Photodegradation of tartrazine dye favored by natural sunlight on pure and (Ce, Ag) co-doped ZnO catalysts. Water Sci Technol 83:2118–2134. https://doi.org/10.2166/wst.2021.106

Bouarroudj T, Aoudjit L, Nessaibia I et al (2023) Enhanced Photocatalytic Activity of Ce and Ag Co-Doped ZnO Nanorods of Paracetamol and Metronidazole Antibiotics Co-Degradation in Wastewater Promoted by Solar Light. Russ J Phys Chem 97:1074–1087. https://doi.org/10.1134/S0036024423050278

Boudiaf M, Messai Y, Bentouhami E et al (2021) Green synthesis of NiO nanoparticles using Nigella sativa extract and their enhanced electrocatalytic activity for the 4-nitrophenol degradation. J Phys Chem Solids 153:110020. https://doi.org/10.1016/j.jpcs.2021.110020

Boulkroune R, Sebais M, Messai Y et al (2019) Hydrothermal synthesis of strontium-doped ZnS nanoparticles: structural, electronic and photocatalytic investigations. Bull Mater Sci 42:223. https://doi.org/10.1007/s12034-019-1905-2

Bouzid K, Djelloul A, Bouzid N, Bougdira J (2009) Electrical resistivity and photoluminescence of zinc oxide films prepared by ultrasonic spray pyrolysis. Phys Status Solidi (A) Appl Mater Sci 206:106–115. https://doi.org/10.1002/pssa.200824403

Cardinale AM, Alberti S, Reverberi AP et al (2023) Antibacterial and Photocatalytic Activities of LDH-Based Sorbents of Different Compositions. Microorganisms 11:1045. https://doi.org/10.3390/microorganisms11041045

Chakra CS, Rajendar V, Rao KV, Kumar M (2017) Enhanced antimicrobial and anticancer properties of ZnO and TiO2 nanocomposites. 3 Biotech 7:1–8. https://doi.org/10.1007/s13205-017-0731-8

Curcic MG, Stankovic MS, Radojevic ID, Stefanovic OD, Comic LR, Topuzovic MD, Djacic DS, Markovic SD (2012) Biological effects, total phenolic content and flavonoid concentrations of fragrant yellow onion (Allium flavum L.). Med Chem 8:46–51. https://doi.org/10.2174/157340612799278441

da Silva BL, Abuçafy MP, Manaia EB et al (2019) Relationship between structure and antimicrobial activity of zinc oxide nanoparticles: An overview. Int J Nanomed 14:9395–9410. https://doi.org/10.2147/IJN.S216204

Dai Q, Zhang Z, Zhan T et al (2018) Catalytic Ozonation for the Degradation of 5-Sulfosalicylic Acid with Spinel-Type ZnAl2O4 Prepared by Hydrothermal, Sol-Gel, and Coprecipitation Methods: A Comparison Study. ACS Omega 3:6506–6512. https://doi.org/10.1021/acsomega.8b00263

Danial EN, Hjiri M, Abdel-wahab MS et al (2020) Antibacterial activity of In-doped ZnO nanoparticles. Inorg Chem Commun 122:108281. https://doi.org/10.1016/j.inoche.2020.108281

Derewacz DK, Goodwin CR, McNees CR et al (2013) Antimicrobial drug resistance affects broad changes in metabolomic phenotype in addition to secondary metabolism. Proc Natl Acad Sci USA 110:2336–2341. https://doi.org/10.1073/pnas.1218524110

Díez-Pascual AM, Luceño-Sánchez JA (2021) Antibacterial activity of polymer nanocomposites incorporating graphene and its derivatives: A state of art. Polymers 13:2105. https://doi.org/10.3390/polym13132105

Djearamane S, Xiu L-J, Wong L-S et al (2022) Antifungal Properties of Zinc Oxide Nanoparticles on Candida albicans. Coatings 12:1864. https://doi.org/10.3390/coatings12121864

Fymat AL (2017) Antibiotics and Antibiotic Resistance. Biomed J Sci Tech Res 1:1–16. https://doi.org/10.26717/bjstr.2017.01.000117

Ghribi F, Sehailia M, Aoudjit L et al (2020) Solar-light promoted photodegradation of metronidazole over ZnO-ZnAl2O4 heterojunction derived from 2D-layered double hydroxide structure. J Photochem Photobiol, A 397:112510. https://doi.org/10.1016/j.jphotochem.2020.112510

Gunasekera TS, Csonka LN, Paliy O (2008) Genome-wide transcriptional responses of Escherichia coli K-12 to continuous osmotic and heat stresses. J Bacteriol 190:3712–3720. https://doi.org/10.1128/JB.01990-07

Guo BL, Han P, Guo LC et al (2015) The Antibacterial Activity of Ta-doped ZnO Nanoparticles. Nanoscale Res Lett 10:1–10. https://doi.org/10.1186/s11671-015-1047-4

Gupta J, Bahadur D (2018) Defect-Mediated Reactive Oxygen Species Generation in Mg-Substituted ZnO Nanoparticles: Efficient Nanomaterials for Bacterial Inhibition and Cancer Therapy. ACS Omega 3:2956–2965. https://doi.org/10.1021/acsomega.7b01953

Hancock JT, Desikan R, Neill SJ (2001) Role of reactive oxygen species in cell signalling pathways. Biochem Soc Trans 29:345–350. https://doi.org/10.1042/0300-5127:0290345

Hirota K, Sugimoto M, Kato M et al (2010) Preparation of zinc oxide ceramics with a sustainable antibacterial activity under dark conditions. Ceram Int 36:497–506. https://doi.org/10.1016/j.ceramint.2009.09.026

Iaiche S, Djelloul A (2015) ZnO/ZnAl2O4 nanocomposite films studied by X-Ray diffraction, FTIR, and X-Ray photoelectron spectroscopy. J Spectrosc 2015:1–9. https://doi.org/10.1155/2015/836859

Iaiche S, Boukaous C, Alamarguy D et al (2020) Effect of solution concentration on ZnO/ZnAl2O4 nanocomposite thin films formation deposited by ultrasonic spray pyrolysis on glass and si(111) substrates. Journal of Nano Research 63:10–30. https://doi.org/10.4028/www.scientific.net/JNanoR.63.10

Ibrahim NA, Abou Elmaaty TM, Eid BM, Abd El-Aziz E (2013) Combined antimicrobial finishing and pigment printing of cotton/polyester blends. Carbohyd Polym 95:379–388. https://doi.org/10.1016/j.carbpol.2013.02.078

Ibrahim NA, Nada AA, Hassabo AG et al (2017) Effect of different capping agents on physicochemical and antimicrobial properties of ZnO nanoparticles. Chem Pap 71:1365–1375. https://doi.org/10.1007/s11696-017-0132-9

Jones N, Ray B, Ranjit KT, Manna AC (2008) Antibacterial activity of ZnO nanoparticle suspensions on a broad spectrum of microorganisms. FEMS Microbiol Lett 279:71–76. https://doi.org/10.1111/j.1574-6968.2007.01012.x

Juan CA, Pérez De La Lastra JM, Plou FJ, Pérez-Lebeña E (2021) The Chemistry of Reactive Oxygen Species (ROS) Revisited: Outlining Their Role in Biological Macromolecules (DNA, Lipids and Proteins) and Induced Pathologies. IJMS 22:4642. https://doi.org/10.3390/ijms22094642

Kanezaki E (2004) Preparation of layered double hydroxides. Interface Sci Technol 1:345–373. https://doi.org/10.1016/S1573-4285(04)80047-4

Lakshmi Prasanna V, Vijayaraghavan R (2015) Insight into the Mechanism of Antibacterial Activity of ZnO: Surface Defects Mediated Reactive Oxygen Species Even in the Dark. Langmuir 31:9155–9162. https://doi.org/10.1021/acs.langmuir.5b02266

Li M, Zhu L, Lin D (2011) Toxicity of ZnO nanoparticles to escherichia Coli: Mechanism and the influence of medium components. Environ Sci Technol 45:1977–1983. https://doi.org/10.1021/es102624t

Lin YJ, Xu XY, Huang L et al (2009) Bactericidal properties of ZnO-Al2O3 composites formed from layered double hydroxide precursors. J Mater Sci - Mater Med 20:591–595. https://doi.org/10.1007/s10856-008-3585-0

Lupan O, Chow L, Chai G (2009) A single ZnO tetrapod-based sensor. Sens Actuators, B Chem 141:511–517. https://doi.org/10.1016/j.snb.2009.07.011

MacGowan A, Macnaughton E (2017) Antibiotic Resistance. Medicine (united Kingdom) 45:622–628. https://doi.org/10.1016/j.mpmed.2017.07.006

Mager WH, De Boer AH, Siderius MH, Voss HP (2000) Cellular responses to oxidative and osmotic stress. Cell Stress Chaperones 5:73–75. https://doi.org/10.1379/1466-1268(2000)005<0073:crtoao>2.0.co;2

Meena Kumari M, Philip D (2015) Synthesis of biogenic SnO2 nanoparticles and evaluation of thermal, rheological, antibacterial and antioxidant activities. Powder Technol 270:312–319. https://doi.org/10.1016/j.powtec.2014.10.034

Mrabet C, Mahdhi N, Boukhachem A et al (2016) Effects of surface oxygen vacancies content on wettability of zinc oxide nanorods doped with lanthanum. J Alloy Compd 688:122–132. https://doi.org/10.1016/j.jallcom.2016.06.286

Narayana PA, Suryanarayana D, Kevan L (1982) Electron spin-echo studies of the solvation structure of superoxide ion (O2-) in water. J Am Chem Soc 104:3552–3555. https://doi.org/10.1021/ja00377a002

Nath BK, Chaliha C, Kalita E, Kalita MC (2016) Synthesis and characterization of ZnO:CeO2:nanocellulose:PANI bionanocomposite. A bimodal agent for arsenic adsorption and antibacterial action. Carbohyd Polym 148:397–405. https://doi.org/10.1016/j.carbpol.2016.03.091

Nickel NH, Fleischer K (2003) Hydrogen Local Vibrational Modes in Zinc Oxide. Phys Rev Lett 90:4. https://doi.org/10.1103/PhysRevLett.90.197402

Nyambo C, Songtipya P, Manias E et al (2008) Effect of MgAl-layered double hydroxide exchanged with linear alkyl carboxylates on fire-retardancy of PMMA and PS. J Mater Chem 18:4827. https://doi.org/10.1039/b806531d

O'Neill AJ, Chopra I (2004) Preclinical evaluation of novel antibacterial agents by microbiological and molecular techniques. Expert Opin Investig Drugs 13:1045–1063. https://doi.org/10.1517/13543784.13.8.1045

Obeizi Z, Benbouzid H, Bouarroudj T, Bououdina M (2021) Excellent antimicrobial and anti-biofilm activities of Fe-SnO2nanoparticles as promising antiseptics and disinfectants. Adv Nat Sci: Nanosci Nanotechnol 12:15003. https://doi.org/10.1088/2043-6254/abde42

Pan N, Li Z, Ren X, Huang TS (2019) Antibacterial films with enhanced physical properties based on poly (vinyl alcohol) and

halogen aminated-graphene oxide. J Appl Polym Sci 136:1–8. https://doi.org/10.1002/app.48176
Pasquet J, Chevalier Y, Pelletier J et al (2014) The contribution of zinc ions to the antimicrobial activity of zinc oxide. Colloids Surf, A 457:263–274. https://doi.org/10.1016/j.colsurfa.2014.05.057
Pasquet J, Chevalier Y, Couval E et al (2015) Zinc oxide as a new antimicrobial preservative of topical products: Interactions with common formulation ingredients. Int J Pharm 479:88–95. https://doi.org/10.1016/j.ijpharm.2014.12.031
Petkova P, Francesko A, Fernandes MM et al (2014) Sonochemical coating of textiles with hybrid ZnO/chitosan antimicrobial nanoparticles. ACS Appl Mater Interfaces 6:1164–1172. https://doi.org/10.1021/am404852d
Querebillo CJ (2023) A Review on Nano Ti-Based Oxides for Dark and Photocatalysis: From Photoinduced Processes to Bioimplant Applications. Nanomaterials 13:982. https://doi.org/10.3390/nano13060982
Ravichandran K, Rathi R, Baneto M et al (2015) Effect of Fe+F doping on the antibacterial activity of ZnO powder. Ceram Int 41:3390–3395. https://doi.org/10.1016/j.ceramint.2014.10.121
Revelas A (2012) Healthcare - associated infections: A public health problem. Niger Med J 53:59. https://doi.org/10.4103/0300-1652.103543
Salem W, Leitner DR, Zingl FG et al (2015) Antibacterial activity of silver and zinc nanoparticles against Vibrio cholerae and enterotoxic Escherichia coli. Int J Med Microbiol 305:85–95. https://doi.org/10.1016/j.ijmm.2014.11.005
Salima M, Youcef M, Bouarroudj T et al (2023) Sunlight-assisted photocatalytic degradation of tartrazine in the presence of Mg doped ZnS nanocatalysts. Solid State Sci 143:107260. https://doi.org/10.1016/j.solidstatesciences.2023.107260
Sirelkhatim A, Mahmud S, Seeni A et al (2015) Review on zinc oxide nanoparticles: Antibacterial activity and toxicity mechanism. Nano-Micro Letters 7:219–242. https://doi.org/10.1007/s40820-015-0040-x
Slavin YN, Asnis J, Häfeli UO, Bach H (2017) Metal nanoparticles: understanding the mechanisms behind antibacterial activity. J Nanobiotechnol 15:65. https://doi.org/10.1186/s12951-017-0308-z
Stankic S, Suman S, Haque F, Vidic J (2016) Pure and multi metal oxide nanoparticles: Synthesis, antibacterial and cytotoxic properties. Journal of Nanobiotechnology 14:1–20. https://doi.org/10.1186/s12951-016-0225-6
Stoimenov PK, Klinger RL, Marchin GL, Klabunde KJ (2002) Metal oxide nanoparticles as bactericidal agents. Langmuir 18:6679–6686. https://doi.org/10.1021/la0202374
Sunder S, Rohilla S, Kumar S, Aghamkar P (2011) Structural characterization of spinel zinc aluminate nanoparticles prepared by coprecipitation method. AIP Conf Proc 1393:123–124. https://doi.org/10.1063/1.3653640
Suresh S, Saravanan P, Jayamoorthy K et al (2016) Development of silane grafted ZnO core shell nanoparticles loaded diglycidyl epoxy nanocomposites film for antimicrobial applications. Mater Sci Eng, C 64:286–292. https://doi.org/10.1016/j.msec.2016.03.096
Tairi L, Messai Y, Bourzami R et al (2022) Enhanced photoluminescence and photocatalytic activity of Ca2+ addition into ZnS nanoparticles synthesized by hydrothermal method. Physica B 631:413713. https://doi.org/10.1016/j.physb.2022.413713
Touahra F, Sehailia M, Halliche D et al (2016) (MnO/Mn3O4)-NiAl nanoparticles as smart carbon resistant catalysts for the production of syngas by means of CO2 reforming of methane: Advocating the role of concurrent carbothermic redox looping in the elimination of coke. Int J Hydrogen Energy 41:21140–21156. https://doi.org/10.1016/j.ijhydene.2016.08.194
Vallapa N, Wiarachai O, Thongchul N et al (2011) Enhancing antibacterial activity of chitosan surface by heterogeneous quaternization. Carbohyd Polym 83:868–875. https://doi.org/10.1016/j.carbpol.2010.08.075
Vidhu VK, Philip D (2015) Biogenic synthesis of SnO2 nanoparticles: Evaluation of antibacterial and antioxidant activities. Spectrochim Acta Part A Mol Biomol Spectrosc 134:372–379. https://doi.org/10.1016/j.saa.2014.06.131
Vijayaprasath G, Murugan R, Palanisamy S et al (2016) Role of nickel doping on structural, optical, magnetic properties and antibacterial activity of ZnO nanoparticles. Mater Res Bull 76:48–61. https://doi.org/10.1016/j.materresbull.2015.11.053
Vinet L, Zhedanov A (2011) Antimicrobial activity of bleached cattail fibers (Typha domingensis) impregnated with silver nanoparticles and benzalkonium chloride. J Phys a: Math Theor 44:1–13. https://doi.org/10.1088/1751-8113/44/8/085201
Wang SF, Sun GZ, Fang LM et al (2015) A comparative study of ZnAl2O4 nanoparticles synthesized from different aluminum salts for use as fluorescence materials. Sci Rep 5:1–12. https://doi.org/10.1038/srep12849
Wang L, Hu C, Shao L (2017) The antimicrobial activity of nanoparticles: Present situation and prospects for the future. Int J Nanomed 12:1227–1249. https://doi.org/10.2147/IJN.S121956
Yadav S, Mittal A, Sharma S et al (2020) Low temperature synthesized ZnO/Al2O3 nano-composites for photocatalytic and antibacterial applications. Semiconductor Science and Technology 35:055008. https://doi.org/10.1088/1361-6641/ab7776
Yin IX, Zhang J, Zhao IS et al (2020) The Antibacterial Mechanism of Silver Nanoparticles and Its Application in Dentistry. IJN 15:2555–2562. https://doi.org/10.2147/IJN.S246764
You C, Han C, Wang X et al (2012) The progress of silver nanoparticles in the antibacterial mechanism, clinical application and cytotoxicity. Mol Biol Rep 39:9193–9201. https://doi.org/10.1007/s11033-012-1792-8
Yu Z, Li Q, Wang J et al (2020) Reactive Oxygen Species-Related Nanoparticle Toxicity in the Biomedical Field. Nanoscale Res Lett 15:115. https://doi.org/10.1186/s11671-020-03344-7
Zabransky RJ, Johnston JA, Hauser KJ (1973) Bacteriostatic and bactericidal activities of various antibiotics against Bacteroides fragilis. Antimicrob Agents Chemother 3:152–156. https://doi.org/10.1128/AAC.3.2.152
Zhang K, Zhu Y, Liu X et al (2017) Sr/ZnO doped titania nanotube array: An effective surface system with excellent osteoinductivity and self-antibacterial activity. Mater Des 130:403–412. https://doi.org/10.1016/j.matdes.2017.05.085
Zhao SW, Guo CR, Hu YZ et al (2018) The preparation and antibacterial activity of cellulose/ZnO composite: A review. Open Chem 16:9–20. https://doi.org/10.1515/chem-2018-0006

Publisher's Note Springer Nature remains neutral with regard to jurisdictional claims in published maps and institutional affiliations.

Springer Nature or its licensor (e.g. a society or other partner) holds exclusive rights to this article under a publishing agreement with the author(s) or other rightsholder(s); author self-archiving of the accepted manuscript version of this article is solely governed by the terms of such publishing agreement and applicable law.